Performance Analysis of Beamformers Using Generalized Loading of the Covariance Matrix in the Presence of Random Steering Vector Errors

Olivier Besson, *Senior Member, IEEE,* and François Vincent, *Member, IEEE*

***Abstract*—Robust adaptive beamforming is a key issue in array applications where there exist uncertainties about the steering vector of interest. Diagonal loading is one of the most popular techniques to improve robustness. In this paper, we present a theoretical analysis of the signal-to-interference-plus-noise ratio (SINR) for the class of beamformers based on generalized (i.e., not necessarily diagonal) loading of the covariance matrix in the presence of random steering vector errors. A closed-form expression for the SINR is derived that is shown to accurately predict the SINR obtained in simulations. This theoretical formula is valid for any loading matrix. It provides insights into the influence of the loading matrix and can serve as a helpful guide to select it. Finally, the analysis enables us to predict the level of uncertainties up to which robust beamformers are effective and then depart from the optimal SINR.**

***Index Terms*—Diagonal loading, performance analysis, random steering vector errors, robust adaptive beamforming.**

I. Introduction

ADAPTIVE beamforming is a primary task in most systems using an array of sensors, and it has applications in numerous domains, including seismology, sonar, radar, and communications, to name a few [1]–[3]. The optimal beamformer, i.e., the beamformer that maximizes the output signal to interference and noise ratio, is known to be, up to a scaling factor, given by $\boldsymbol{R}^{-1}\boldsymbol{a}$, where $\boldsymbol{R}$ is the covariance matrix of the received signals, and $\boldsymbol{a}$ stands for the steering vector of the signal of interest (SOI). In order to implement the optimal beamformer, $\boldsymbol{a}$ needs to be known precisely, which is a property that is most often not encountered in practice. Indeed, there exist potentially many factors that can contribute to steering vector uncertainties. For instance, the source might undergo local scattering or there can exist uncertainties about its direction of arrival; the propagation medium can be nonhomogeneous or might induce fading. Finally, the array's response might not be known perfectly, e.g., the individual gains and phases or the sensors' locations are not precisely known. These types of errors are especially detrimental when the SOI is present in the data as the latter is considered as an interference and thus tends to be eliminated; see, e.g., [4].

Therefore, robust adaptive beamforming has emerged as a necessary constituent of most systems using an array of sensors. See [1] and [5] and references therein for comprehensive overviews. The most widely used method, due to its simplicity and effectiveness, is diagonal loading [6], [7], which consists of adding a scaled identity matrix to the covariance matrix prior to inversion. Diagonal loading can either be viewed as a means to "equalize" the least significant eigenvalues of the sample covariance matrix [8, p. 666] or to constrain the white noise array gain [1, ch. 6], [9]. The latter interpretation also suggests that it can be effective when dealing with uncalibrated arrays [1, ch. 6]. Interestingly enough, diagonal loading turns out to be the solution to worst-case approaches recently proposed in [10]–[12]. In the latter references, the beamformer is designed to minimize the output power subject to the constraint that the beamformer's response be above some level for all the steering vectors that lie in an ellipsoid centered around the nominal or presumed steering vector of interest. This guarantees that the signal of interest, whose steering vector is expected to lie in the ellipsoid, will not be eliminated, and hence, robustness is improved. When the ellipsoid is a sphere, then the solution to the above-mentioned problem is of the diagonal loading type, where the loading level is obtained from a secular equation involving the covariance matrix and the radius of the sphere. In the case where the ellipsoid is not a sphere or is flat, the robust beamformer takes the form of a general (i.e., not necessarily diagonal) loading of the covariance matrix. In either case, the solution is given by $(\boldsymbol{R}+\boldsymbol{Q})^{-1}\overline{\boldsymbol{a}}$, where $\overline{\boldsymbol{a}}$ denotes the nominal steering vector (in the absence of any uncertainty), and $\boldsymbol{Q}$ stands for the loading matrix.

Through numerical simulations, this robust adaptive beamformer was shown to perform well, at least when the size of the ellipsoid does not grow large. However, no theoretical analysis was provided and assessing its performance remains an open problem. The finite-sample SINR analysis of the minimum variance distortionless response (MVDR) beamformer was presented in the famous paper by Reed *et al.* [13], where the probability density function (pdf) of the SINR loss (compared to perfectly known interference plus noise covariance matrix) is derived; see also [14] and [15] for alternate derivations. Similar finite-sample SINR's probability density function (pdf) analysis for minimum power distortionless response (MPDR) beamformer, i.e., when the signal of interest is present in the measurements, are reported in [16] and [17]. In the latter reference, Boroson also considered the case where the steering vector used in the computation of the MPDR weight vector differs from the actual steering vector. A complete finite-sample analysis of the MPDR SINR is also presented in [18] (with an extension in [19], where the combined effects of steering vector and finite-sample

Manuscript received Oct. 10, 2003; revised March 4, 2004. The associate editor coordinating the review of this paper and approving it for publication was Dr. Alex B. Gershman.

The authors are with the Department of Avionics and Systems, ENSICA, 31056 Toulouse, France (e-mail: besson@ensica.fr; vincent@ensica.fr).

Digital Object Identifier 10.1109/TSP.2004.840777

errors are studied) when the signal and interferences are possibly correlated. In-depth statistical analysis of the pdf of the signal waveform estimator and weight vector can be found in [20] and [21] for a large class of beamformers. In contrast, analysis of diagonally loaded versions of the MPDR is scarce. A large-sample analysis of the weight vector and powers at the output of a diagonally loaded MPDR can be found in [22] and [23], whereas [24] derives the pdf of the beam response when diagonal loading is used. In this paper, we present a theoretical analysis of the SINR obtained with a general fixed loading matrix and in the presence of random steering vector uncertainties. The formulas obtained are quite simple and are valid for any loading matrix $\boldsymbol{Q}$ (including nondiagonal or noninvertible). Additionally, they are shown to predict well the performances obtained via numerical simulations. Finally, they can serve to provide insights into the choice of the loading matrix.

II. Data Model

We consider an array composed of m sensors and assume that the array's output can be written as

$$\boldsymbol{x}_t = \boldsymbol{a}s_t + \boldsymbol{n}_t \quad t = 1, \cdots, N \tag{1}$$

where $\boldsymbol{a}$ is the actual steering vector of the source of interest, s_t is the corresponding emitted signal, and $\boldsymbol{n}_t$ denotes the noise contribution (possibly including interferences). We assume the following.

- $\boldsymbol{a}$ is a complex-valued, circularly symmetric (i.e., $\mathcal{E}\{(\boldsymbol{a}-\overline{\boldsymbol{a}})(\boldsymbol{a}-\overline{\boldsymbol{a}})^T\} = \boldsymbol{0}$) random vector with mean and covariance matrix given, respectively, by

$$\begin{aligned} \mathcal{E}\{\boldsymbol{a}\} &= \overline{\boldsymbol{a}} \\ \mathcal{E}\left\{(\boldsymbol{a}-\overline{\boldsymbol{a}})(\boldsymbol{a}-\overline{\boldsymbol{a}})^H\right\} &= \boldsymbol{C}_a. \end{aligned} \tag{2}$$

  $\overline{\boldsymbol{a}}$ corresponds to the steering vector without any perturbation (e.g., for a perfectly calibrated array), whereas $\boldsymbol{C}_a$ captures the effects of all possible errors affecting the steering vector.
- $\boldsymbol{n}_t$ is the noise contribution, including interferences and thermal noise. $\boldsymbol{n}_t$ is assumed to be drawn from a zero-mean complex-valued Gaussian distribution with covariance matrix $\boldsymbol{C}$.
- s_t is a zero-mean random process with power $P = \mathcal{E}\{|s_t|^2\}$.

The robust adaptive beamformers of [10]–[12] (although their formulations are different) are obtained as the solution to the following minimization problem:

$$\begin{aligned} \min_{\boldsymbol{w}} \boldsymbol{w}^H\boldsymbol{R}\boldsymbol{w} \text{ subject to } &|\boldsymbol{w}^H\boldsymbol{a}| \geq 1 \\ &\forall \boldsymbol{a} = \overline{\boldsymbol{a}} + \boldsymbol{B}\boldsymbol{u};\ \|\boldsymbol{u}\| \leq 1 \end{aligned} \tag{3}$$

where $\boldsymbol{B}$ is a $m \times r$ matrix with full column rank, which defines an ellipsoid centered around $\overline{\boldsymbol{a}}$. Under mild assumptions, the solution to (3) is given by (up to a scaling factor that does not affect the SINR)

$$\boldsymbol{w} = (\boldsymbol{R}+\boldsymbol{Q})^{-1}\overline{\boldsymbol{a}} \tag{4}$$

with $\boldsymbol{Q} = \lambda(\overline{\boldsymbol{a}}, \boldsymbol{R})\boldsymbol{B}\boldsymbol{B}^H$ and where the Lagrange multiplier $\lambda(\overline{\boldsymbol{a}}, \boldsymbol{R})$ is obtained as the solution of a secular equation that involves $\boldsymbol{B}^H\boldsymbol{R}^{-1}\overline{\boldsymbol{a}}$ and the eigenvalue decomposition of $\boldsymbol{B}^H\boldsymbol{R}^{-1}\boldsymbol{B}$; see [10] for details. Observe that the loading level $\lambda(\overline{\boldsymbol{a}}, \boldsymbol{R})$ is chosen adaptively, i.e., it depends on the covariance matrix while the shaping matrix $\boldsymbol{B}\boldsymbol{B}^H$ is fixed. When $\boldsymbol{B} = \boldsymbol{I}$, the ellipsoid becomes a sphere, and the solution amounts to conventional diagonal loading.

In this paper, we present a SINR analysis of the robust beamformer (4) in the case where $\boldsymbol{Q} = \lambda\overline{\boldsymbol{Q}}$ and both λ and $\overline{\boldsymbol{Q}}$ are fixed. Therefore, the analysis does not apply directly to [10]–[12], where the loading level depends on the scenario via the covariance matrix. We will study the influence of both the shaping matrix $\overline{\boldsymbol{Q}}$ and the loading level λ by varying these parameters. A two-step procedure is taken to perform the analysis. First, we provide an expression of the SINR for a given $\boldsymbol{a}$. Then, this SINR is averaged over the pdf of $\boldsymbol{a}$ to yield the average SINR. Note that here, we do not consider finite-sample effects, i.e., we assume that the true covariance matrix (for a given $\boldsymbol{a}$) $\boldsymbol{R}$ is available. In order to introduce finite-sample effects (and thereby to combine them with steering vector errors), one needs to assume that the two errors are of the same order of magnitude; otherwise, one type of error dominates and the analysis boils down to finite-sample only or steering vector errors only analysis. In our case, since the errors in estimating $\boldsymbol{R}$ are $O(1/N)$, this would amount to assuming that $\boldsymbol{C}_a = \overline{\boldsymbol{C}}_a/N$, where $\overline{\boldsymbol{C}}_a$ is fixed, and N denotes the number of snapshots. See [25] and [26] for a detailed and comprehensive discussion on this issue. However, this assumption may seem arbitrary since the errors are not likely to depend on N. Therefore, herein, we consider that N is large enough so that the steering vector errors dominate. We will however illustrate the finite-sample behavior of (4) in the numerical simulations. Before closing this section, we would like to point out that the loading-based beamformer in (4) might not be the most appropriate solution under the stated hypotheses. Indeed, the approaches proposed in [27] that consider robustness against errors in the SOI covariance matrix are suitable in our case since the SOI covariance matrix is $P_s(\overline{\boldsymbol{a}}\overline{\boldsymbol{a}}^H + \boldsymbol{C}_a)$ and differs from the "nominal" covariance matrix $P_s\overline{\boldsymbol{a}}\overline{\boldsymbol{a}}^H$. However, analysis of the beamformers in [27] is beyond the scope of the present paper, where we focus on beamformers of the type (4).

III. SINR Analysis

In this section, we provide a theoretical expression for the average SINR when the weight vector is computed, as in (4), and the steering vector is random with mean and covariance matrix given by (2). We proceed as follows. In a first step, we assume that $\boldsymbol{a}$ is given and derive the corresponding SINR. Then, we invoke the conditional expectation rule to compute the average SINR as

$$\overline{\text{SINR}} = \mathcal{E}_{\boldsymbol{a}}\{\text{SINR}_{|\boldsymbol{a}}\} \tag{5}$$

where $\mathcal{E}_{\boldsymbol{a}}\{.\}$ denotes the expectation with respect to (w.r.t.) the pdf of $\boldsymbol{a}$, and $\text{SINR}_{|\boldsymbol{a}}$ corresponds to the SINR for a given $\boldsymbol{a}$. In

order to obtain $\text{SINR}_{|\boldsymbol{a}}$, note that the weight vector, for a given $\boldsymbol{a}$, is given by

$$\boldsymbol{w}_{|\boldsymbol{a}} = (\boldsymbol{R}_{|\boldsymbol{a}} + \boldsymbol{Q})^{-1}\overline{\boldsymbol{a}} \tag{6}$$

where $\boldsymbol{R}_{|\boldsymbol{a}}$ denotes the covariance matrix for a given $\boldsymbol{a}$. Therefore

$$\begin{aligned}\text{SINR}_{|\boldsymbol{a}} &= \frac{P\left|\boldsymbol{w}_{|\boldsymbol{a}}^H \boldsymbol{a}\right|^2}{\boldsymbol{w}_{|\boldsymbol{a}}^H \boldsymbol{C} \boldsymbol{w}_{|\boldsymbol{a}}} \\ &= \frac{P\left|\overline{\boldsymbol{a}}^H (\boldsymbol{R}_{|\boldsymbol{a}} + \boldsymbol{Q})^{-1}\boldsymbol{a}\right|^2}{\overline{\boldsymbol{a}}^H (\boldsymbol{R}_{|\boldsymbol{a}} + \boldsymbol{Q})^{-1}\boldsymbol{C}(\boldsymbol{R}_{|\boldsymbol{a}} + \boldsymbol{Q})^{-1}\overline{\boldsymbol{a}}}.\end{aligned} \tag{7}$$

However, using (1) along with the stated assumptions, it follows that the covariance matrix is given by

$$\boldsymbol{R}_{|\boldsymbol{a}} = P\boldsymbol{a}\boldsymbol{a}^H + \boldsymbol{C}. \tag{8}$$

Let $\widetilde{\boldsymbol{Q}} = \boldsymbol{Q} + \boldsymbol{C}$. Using Woodbury's identity, it can be shown that

$$(\boldsymbol{R}_{|\boldsymbol{a}} + \boldsymbol{Q})^{-1}\boldsymbol{a} = \frac{\widetilde{\boldsymbol{Q}}^{-1}\boldsymbol{a}}{1 + P\boldsymbol{a}^H\widetilde{\boldsymbol{Q}}^{-1}\boldsymbol{a}} \tag{9a}$$

$$(\boldsymbol{R}_{|\boldsymbol{a}} + \boldsymbol{Q})^{-1}\overline{\boldsymbol{a}} = \widetilde{\boldsymbol{Q}}^{-1}\left(\overline{\boldsymbol{a}} - \frac{P\boldsymbol{a}^H\widetilde{\boldsymbol{Q}}^{-1}\overline{\boldsymbol{a}}}{1 + P\boldsymbol{a}^H\widetilde{\boldsymbol{Q}}^{-1}\boldsymbol{a}}\boldsymbol{a}\right). \tag{9b}$$

Therefore, after some straightforward algebraic manipulations, we obtain the following expression for the SINR for a given $\boldsymbol{a}$:

$$\text{SINR}_{|\boldsymbol{a}} = \frac{1}{P\,(\boldsymbol{a} - \gamma(\boldsymbol{a})\overline{\boldsymbol{a}})^H\,\boldsymbol{Z}\,(\boldsymbol{a} - \gamma(\boldsymbol{a})\overline{\boldsymbol{a}})} \tag{10}$$

where

$$\begin{aligned}\gamma(\boldsymbol{a}) &= \frac{1 + P\boldsymbol{a}^H\widetilde{\boldsymbol{Q}}^{-1}\boldsymbol{a}}{P\boldsymbol{a}^H\widetilde{\boldsymbol{Q}}^{-1}\overline{\boldsymbol{a}}} \\ \boldsymbol{Z} &= \widetilde{\boldsymbol{Q}}^{-1}\boldsymbol{C}\widetilde{\boldsymbol{Q}}^{-1}.\end{aligned} \tag{11}$$

The average SINR is thus given by

$$\overline{\text{SINR}} = \int \frac{p(\boldsymbol{a})}{P\,(\boldsymbol{a} - \gamma(\boldsymbol{a})\overline{\boldsymbol{a}})^H\,\boldsymbol{Z}\,(\boldsymbol{a} - \gamma(\boldsymbol{a})\overline{\boldsymbol{a}})}d\boldsymbol{a} \tag{12}$$

where $p(\boldsymbol{a})$ is the pdf of $\boldsymbol{a}$. Obtaining a closed-form expression for the previous integral appears to be an intractable task. Hence, we prefer to approximate this integral. In the Appendix, it is shown that for any scalar function $f(\boldsymbol{a})$ and assuming that $\boldsymbol{a}$ is circularly symmetric

$$\int f(\boldsymbol{a})p(\boldsymbol{a})d\boldsymbol{a} \simeq f(\overline{\boldsymbol{a}}) + \text{Tr}\left\{\left.\frac{\partial^2 f}{\partial\boldsymbol{a}\partial\boldsymbol{a}^H}\right|_{\overline{\boldsymbol{a}}}\boldsymbol{C}_a\right\} \tag{13}$$

where $\text{Tr}\{.\}$ stands for the trace of the matrix between braces, and $(\partial^2 f/\partial\boldsymbol{a}\partial\boldsymbol{a}^H)|_{\overline{\boldsymbol{a}}}$ denotes the Hessian of $f(\boldsymbol{a})$ evaluated at $\overline{\boldsymbol{a}}$. It should be pointed out that the previous approximation does not require complete knowledge of the pdf of $\boldsymbol{a}$ but only its mean and covariance matrix, which is an appealing feature. We now apply the result (13) to $\text{SINR}_{|\boldsymbol{a}}$. However, for the purpose of simplifying subsequent derivations, we first simplify the expression of $\text{SINR}_{|\boldsymbol{a}}$ by approximating $\gamma(\boldsymbol{a})$. More precisely, we propose to approximate $\gamma(\boldsymbol{a})$ by its statistical mean. Toward this end, observe that

$$\frac{\partial\gamma}{\partial\boldsymbol{a}} = \frac{\widetilde{\boldsymbol{Q}}^{-1}(\boldsymbol{a} - \gamma\overline{\boldsymbol{a}})}{\boldsymbol{a}^H\widetilde{\boldsymbol{Q}}^{-1}\overline{\boldsymbol{a}}} \tag{14a}$$

$$\frac{\partial^2\gamma}{\partial\boldsymbol{a}\partial\boldsymbol{a}^H} = \frac{\widetilde{\boldsymbol{Q}}^{-1}}{\boldsymbol{a}^H\widetilde{\boldsymbol{Q}}^{-1}\overline{\boldsymbol{a}}}\left(\boldsymbol{I} - \frac{\overline{\boldsymbol{a}}\boldsymbol{a}^H\widetilde{\boldsymbol{Q}}^{-1}}{\boldsymbol{a}^H\widetilde{\boldsymbol{Q}}^{-1}\overline{\boldsymbol{a}}}\right) \tag{14b}$$

where, to obtain (14), we used the fact that

$$\frac{\partial\boldsymbol{a}^H\widetilde{\boldsymbol{Q}}^{-1}\boldsymbol{a}}{\partial\boldsymbol{a}} = \widetilde{\boldsymbol{Q}}^{-1}\boldsymbol{a}; \quad \frac{\partial\boldsymbol{a}^H\widetilde{\boldsymbol{Q}}^{-1}\overline{\boldsymbol{a}}}{\partial\boldsymbol{a}} = \widetilde{\boldsymbol{Q}}^{-1}\overline{\boldsymbol{a}} \tag{15a}$$

$$\frac{\partial\widetilde{\boldsymbol{Q}}^{-1}\boldsymbol{a}}{\partial\boldsymbol{a}^H} = \widetilde{\boldsymbol{Q}}^{-1}; \quad \frac{\partial\boldsymbol{a}^H\widetilde{\boldsymbol{Q}}^{-1}\overline{\boldsymbol{a}}}{\partial\boldsymbol{a}^H} = \boldsymbol{0}. \tag{15b}$$

Reporting (14) in (13) yields

$$\begin{aligned}\mathcal{E}_{\boldsymbol{a}}\{\gamma(\boldsymbol{a})\} &\simeq \frac{1 + P\overline{\boldsymbol{a}}^H\widetilde{\boldsymbol{Q}}^{-1}\overline{\boldsymbol{a}}}{P\overline{\boldsymbol{a}}^H\widetilde{\boldsymbol{Q}}^{-1}\overline{\boldsymbol{a}}} + \frac{\text{Tr}\{\widetilde{\boldsymbol{Q}}^{-1}\boldsymbol{C}_a\}}{\overline{\boldsymbol{a}}^H\widetilde{\boldsymbol{Q}}^{-1}\overline{\boldsymbol{a}}} \\ &\quad - \frac{\overline{\boldsymbol{a}}^H\widetilde{\boldsymbol{Q}}^{-1}\boldsymbol{C}_a\widetilde{\boldsymbol{Q}}^{-1}\overline{\boldsymbol{a}}}{\left(\overline{\boldsymbol{a}}^H\widetilde{\boldsymbol{Q}}^{-1}\overline{\boldsymbol{a}}\right)^2} \\ &\triangleq \gamma_0.\end{aligned} \tag{16}$$

We propose to replace $\gamma(\boldsymbol{a})$ by γ_0 in (10) so that

$$\text{SINR}_{|\boldsymbol{a}} \simeq \frac{1}{P(\boldsymbol{a} - \gamma_0\overline{\boldsymbol{a}})^H\boldsymbol{Z}(\boldsymbol{a} - \gamma_0\overline{\boldsymbol{a}})}. \tag{17}$$

We would like to point out that using γ_0 in lieu of $\gamma(\boldsymbol{a})$ in (13) does not result in a less-accurate expression for the average SINR, as will be illustrated below. The average SINR is thus approximated by

$$\overline{\text{SINR}} \simeq \int \frac{p(\boldsymbol{a})}{P(\boldsymbol{a} - \gamma_0\overline{\boldsymbol{a}})^H\boldsymbol{Z}(\boldsymbol{a} - \gamma_0\overline{\boldsymbol{a}})}d\boldsymbol{a}. \tag{18}$$

Let $f(\boldsymbol{a}) = (\boldsymbol{a} - \gamma_0\overline{\boldsymbol{a}})^H\boldsymbol{Z}(\boldsymbol{a} - \gamma_0\overline{\boldsymbol{a}})$ so that $\text{SINR}_{|\boldsymbol{a}} \simeq [Pf(\boldsymbol{a})]^{-1}$. Using

$$\frac{\partial f}{\partial\boldsymbol{a}} = \boldsymbol{Z}(\boldsymbol{a} - \gamma_0\overline{\boldsymbol{a}}) \tag{19a}$$

$$\frac{\partial^2 f}{\partial\boldsymbol{a}\partial\boldsymbol{a}^H} = \boldsymbol{Z} \tag{19b}$$

along with (13) and (18) yields the following expression:

$$\begin{aligned}\overline{\text{SINR}} &\simeq \frac{1}{P|1 - \gamma_0|^4(\overline{\boldsymbol{a}}^H\boldsymbol{Z}\overline{\boldsymbol{a}})^2} \\ &\quad \times \left\{|1 - \gamma_0|^2(\overline{\boldsymbol{a}}^H\boldsymbol{Z}\overline{\boldsymbol{a}}) - \text{Tr}\{\boldsymbol{Z}\boldsymbol{C}_a\} + 2\frac{\overline{\boldsymbol{a}}^H\boldsymbol{Z}\boldsymbol{C}_a\boldsymbol{Z}\overline{\boldsymbol{a}}}{\overline{\boldsymbol{a}}^H\boldsymbol{Z}\overline{\boldsymbol{a}}}\right\}.\end{aligned} \tag{20}$$

The previous equation provides a closed-form and compact expression for the average SINR. We stress the fact that it holds for a large class of robust adaptive beamformers as it holds for any

loading matrix $\boldsymbol{Q}$ and any steering vector error covariance matrix $\boldsymbol{C}_a$. As will be illustrated in the next section, it predicts very accurately the average SINR obtained through Monte Carlo simulations. Hence, it can serve as a useful tool to obtain rapid insights into the choice of the loading matrix $\boldsymbol{Q}$ without resorting to extensive simulations.

IV. Numerical Illustrations

The aim of this section is threefold. First, we assess the validity of the theoretical formula (20) by comparing it with the actual SINR obtained through Monte Carlo simulations. Second, we provide illustrations of up to which level of uncertainty generalized loading can compensate for steering vector errors and still provide a performance close to optimum. Third, we provide rules of thumb for selecting the shape and the size of the loading matrix. In all simulations, we consider a uniform linear array of $m = 10$ sensors spaced a half-wavelength apart. The signal of interest impinges from broadside, and thus, $\overline{\boldsymbol{a}} = [1 \;\; 1 \;\; \cdots \;\; 1]^T$. We consider two cases for the steering vector errors corresponding to two different matrices $\boldsymbol{C}_a$:

- **Case 1**: The steering vector errors are assumed to be drawn from a zero-mean complex-valued Gaussian distribution with covariance matrix $\boldsymbol{C}_a = \sigma_a^2 \boldsymbol{I}$.
- **Case 2**: We consider the case of local scattering for which the steering vector can be written as

$$\boldsymbol{a} = \overline{\boldsymbol{a}} + \frac{1}{\sqrt{L}} \sum_{k=1}^{L} g_k \boldsymbol{a}(\widetilde{\theta}_k) \tag{21}$$

where g_k are zero-mean, independent, and identically distributed random variables with power σ_g^2, and $\widetilde{\theta}_k$ are independent random variables with pdf $p(\widetilde{\theta})$. The covariance matrix of the errors is given by [28]

$$\boldsymbol{C}_a = \sigma_g^2 \int \boldsymbol{a}(\widetilde{\theta}) \boldsymbol{a}^H(\widetilde{\theta}) p(\widetilde{\theta}) d\widetilde{\theta} = \sigma_g^2 \breve{\boldsymbol{C}}_a. \tag{22}$$

In the simulations presented below, we assume a Gaussian distribution for the scatterers with standard deviation (referred to as angular spread in the literature) $\sigma_\theta = 15^\circ$, and the number of scatterers is set to $L = 10$.

In either case, we define the *uncertainty ratio* (UR) as

$$\mathrm{UR} = 10 \log_{10} \left(\frac{\mathrm{Tr}\{\boldsymbol{C}_a\}}{\overline{\boldsymbol{a}}^H \overline{\boldsymbol{a}}} \right).$$

In all simulations, we consider that the noise component consists of a white noise contribution with power σ_n^2 and two interferences whose DOAs are -20° and 30° and whose powers are 20 and 30 dB above the white noise level, respectively. The signal-to-noise ratio (SNR) is defined as

$$\mathrm{SNR} = 10 \log_{10} \left(\frac{P \left(\overline{\boldsymbol{a}}^H \overline{\boldsymbol{a}} + \mathrm{Tr}\{\boldsymbol{C}_a\} \right)}{\sigma_n^2} \right)$$

and corresponds to an *average array SNR*. In all simulations, the SINR is evaluated as follows. We run $N_r = 500$ Monte Carlo simulations with a different random $\boldsymbol{a}$ drawn from (2), and, for a given weight vector $\boldsymbol{w}$, the average SINR is computed as

$$\overline{\mathrm{SINR}}(\boldsymbol{w}) = \frac{1}{N_r} \sum_{n=1}^{N_r} \frac{P \left| \boldsymbol{w}^H \boldsymbol{a}(n) \right|^2}{\boldsymbol{w}^H \boldsymbol{C} \boldsymbol{w}}. \tag{23}$$

We stress the fact that the measure of performance in (23) is an *average SINR*. In addition to the robust adaptive beamformer (6)—which is referred to as RB in the figures—the following beamformers are tested:

- a (generalized) MVDR beamformer [27] that is given by

$$\begin{aligned} \boldsymbol{w}_{\mathrm{MVDR}} &= \arg\max_{\boldsymbol{w}} \frac{\mathcal{E}\left\{ \left| \boldsymbol{w}^H \boldsymbol{a} s_t \right|^2 \right\}}{\mathcal{E}\left\{ \left| \boldsymbol{w}^H \boldsymbol{n}_t \right|^2 \right\}} \\ &= \arg\max_{\boldsymbol{w}} \frac{\boldsymbol{w}^H (\overline{\boldsymbol{a}}\overline{\boldsymbol{a}}^H + \boldsymbol{C}_a) \boldsymbol{w}}{\boldsymbol{w}^H \boldsymbol{C} \boldsymbol{w}} \\ &= \mathcal{P}\left\{ \boldsymbol{C}^{-1} (\overline{\boldsymbol{a}}\overline{\boldsymbol{a}}^H + \boldsymbol{C}_a) \right\} \end{aligned} \tag{24}$$

where $\mathcal{P}\{.\}$ stands for the principal eigenvector of the matrix between braces. The average SINR associated with the MVDR beamformer is readily obtained as

$$\begin{aligned} \overline{\mathrm{SINR}}_{\mathrm{MVDR}} &= \mathcal{E}_{\boldsymbol{a}} \left\{ \frac{P \left| \boldsymbol{w}_{\mathrm{MVDR}}^H \boldsymbol{a} \right|^2}{\boldsymbol{w}_{\mathrm{MVDR}}^H \boldsymbol{C} \boldsymbol{w}_{\mathrm{MVDR}}} \right\} \\ &= P \lambda_{\max} \left\{ \boldsymbol{C}^{-1} (\overline{\boldsymbol{a}}\overline{\boldsymbol{a}}^H + \boldsymbol{C}_a) \right\} \end{aligned} \tag{25}$$

where $\lambda_{\max}\{.\}$ corresponds to the maximum eigenvalue.

- a (hypothetical) clairvoyant optimum beamformer that maximizes the SINR for any given $\boldsymbol{a}$ and is thus given by

$$\boldsymbol{w}_{|\boldsymbol{a}}^{\mathrm{opt}} = \boldsymbol{C}^{-1} \boldsymbol{a}. \tag{26}$$

The corresponding average SINR is given by

$$\begin{aligned} \overline{\mathrm{SINR}}_{\mathrm{opt}} &= \int P (\boldsymbol{a}^H \boldsymbol{C}^{-1} \boldsymbol{a}) p(\boldsymbol{a}) d\boldsymbol{a} \\ &= P \mathrm{Tr}\left\{ \boldsymbol{C}^{-1} (\overline{\boldsymbol{a}}\overline{\boldsymbol{a}}^H + \boldsymbol{C}_a) \right\}. \end{aligned} \tag{27}$$

Comparing (25) with (27), it immediately follows that $\overline{\mathrm{SINR}}_{\mathrm{opt}} \geq \overline{\mathrm{SINR}}_{\mathrm{MVDR}}$. Note, however, that (27) is really an upper bound and cannot be attained unless $\boldsymbol{a}$ is known; see (26). The robust beamformer (6) will be compared to these two beamfomers in order to see if loading can compensate for steering vector uncertainties and still maintain a performance close to optimum.

- the sample covariance matrix (SCM) version of (6), i.e.,

$$\boldsymbol{w}_{\mathrm{SCM}} = (\widehat{\boldsymbol{R}} + \boldsymbol{Q})^{-1} \overline{\boldsymbol{a}} \tag{28a}$$

$$\widehat{\boldsymbol{R}} = \frac{1}{N} \sum_{t=1}^{N} \boldsymbol{x}_t \boldsymbol{x}_t^H. \tag{28b}$$

The performance of the SCM robust beamformer will be evaluated by (23). It will enable us to take into account finite-sample effects.

In a first series of simulations, we study the performance of the beamformers versus the uncertainty ratio. The loading matrix $\boldsymbol{Q} = \lambda \boldsymbol{I}$, and we define the loading level (LL) as LL=

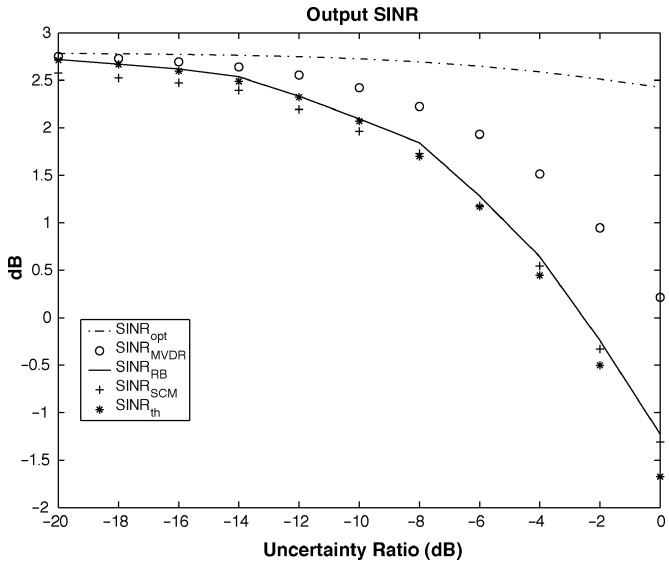

Fig. 1. Case 1—Output SINR versus uncertainty ratio. $m = 10$, SNR $= 3$ dB, LL $= 5$ dB, and $N = 200$. $\boldsymbol{Q} \propto \boldsymbol{I}$.

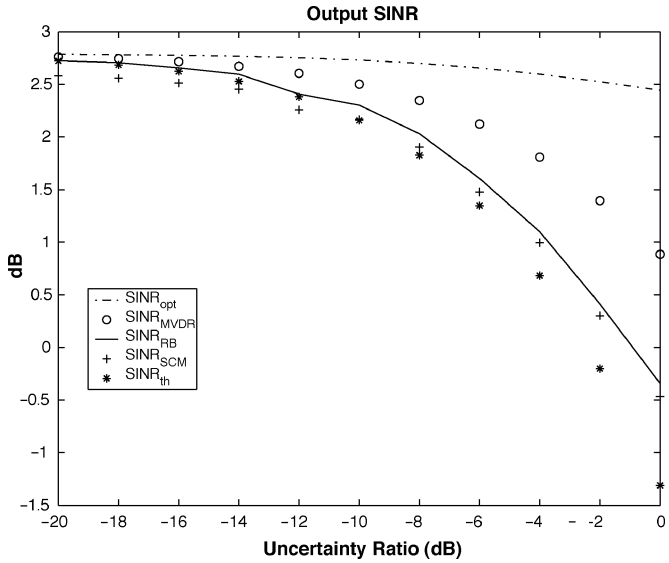

Fig. 2. Case 2—Output SINR versus uncertainty ratio. $m = 10$, SNR $= 3$ dB, LL $= 5$ dB, and $N = 200$. $\boldsymbol{Q} \propto \boldsymbol{I}$.

$10\log_{10}(\lambda/\sigma_n^2)$. Note that it corresponds to a loading level relative to the white noise power. In the simulations, LL is chosen as LL$= 5$ dB. The results are displayed in Figs. 1 and 2. The following observations are in order.

- The theoretical formula (20) is seen to predict very accurately the average SINR obtained in simulations to within 0.2–0.4 dB for UR ≤ -2 dB. Notice that UR $= -2$ dB corresponds to a high uncertainty as the standard deviation of the steering vector error is in this case about 79% of the value of the steering vector. Hence, (20) provides a very good picture of the robust adaptive beamformer's performance in most situations. Moreover, the finite-sample behavior of the robust beamformer is also close to the theoretical formula.
- The robust beamformer has a performance very close to that of the MVDR; the difference is less than 1 dB for URs below -5 dB. For a higher UR, the robust beamformer can no longer compensate for the uncertainties; hence, one must turn to other solutions. It should be pointed out that for UR ≥ -6 dB, the MVDR does not perform as well as the clairvoyant beamformer. Since the latter makes use of the actual steering vector, this suggests that for high uncertainties, the remedy would be to obtain additional information about the actual steering vector, for instance, by estimating it, rather than to protect the array's response over a larger and larger ellipsoid.

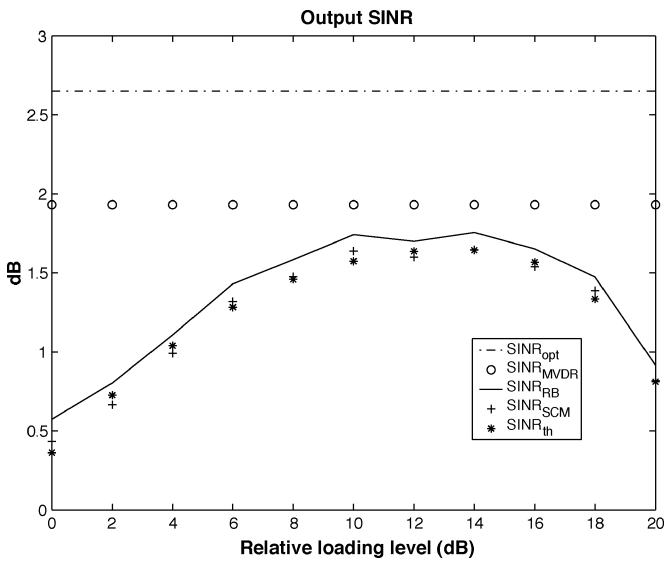

Fig. 3. Case 1-Output SINR versus loading level. $m = 10$, SNR $= 3$ dB, UR $= -6$ dB, and $N = 200$. $\boldsymbol{Q} \propto \boldsymbol{I}$.

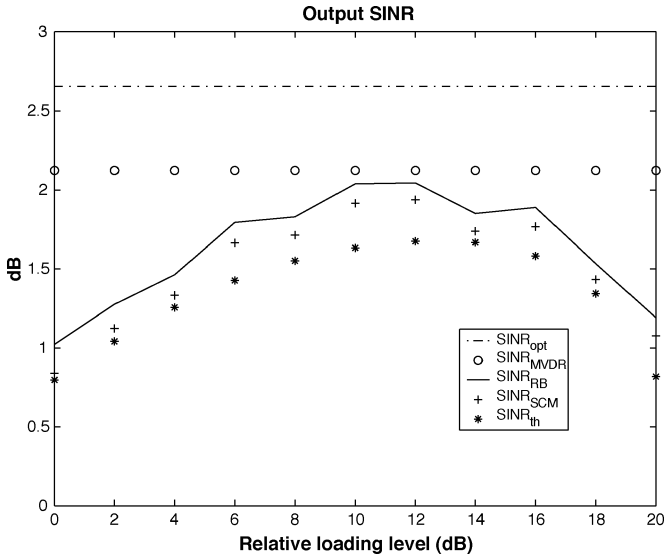

Fig. 4. Case 2—Output SINR versus loading level. $m = 10$, SNR $= 3$ dB, UR $= -6$ dB, and $N = 200$. $\boldsymbol{Q} \propto \boldsymbol{I}$.

Next, the influence of the loading level is studied in Figs. 3 and 4. In these figures, the loading matrix is still proportional to the identity matrix and UR $= -6$ dB. Again, it can be seen that the theoretical average SINR is very close to the practical average SINR. In addition, it can be observed that, although LL has an influence onto the final SINR, there exists a large range of values for LL, which provide a similar performance.

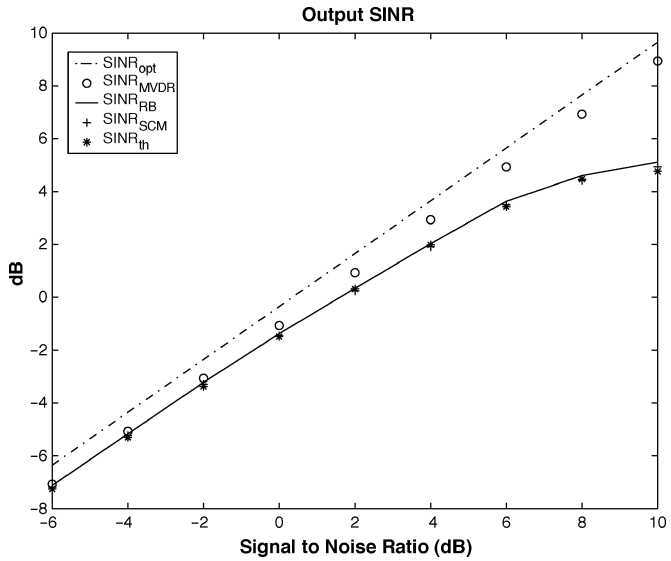

Fig. 5. Case 1—Output SINR versus SNR. $m = 10$, UR $= -6$ dB, and $N = 200$. $\boldsymbol{Q} \propto \boldsymbol{I}$.

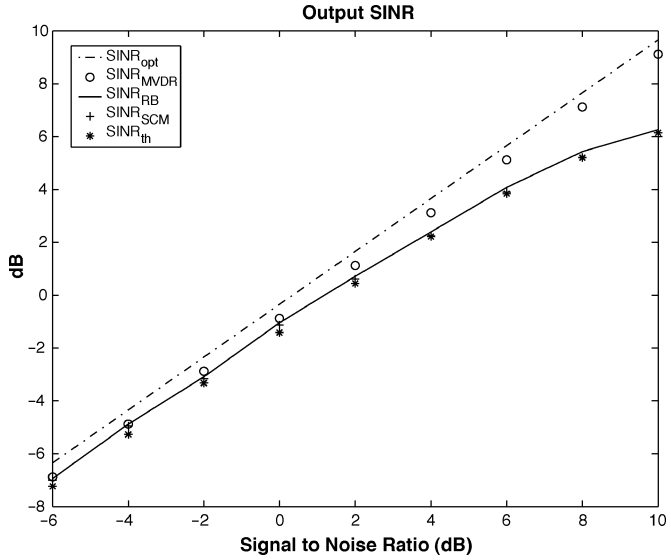

Fig. 6. Case 2—Output SINR versus SNR. $m = 10$, UR $= -6$ dB, and $N = 200$. $\boldsymbol{Q} \propto \boldsymbol{I}$.

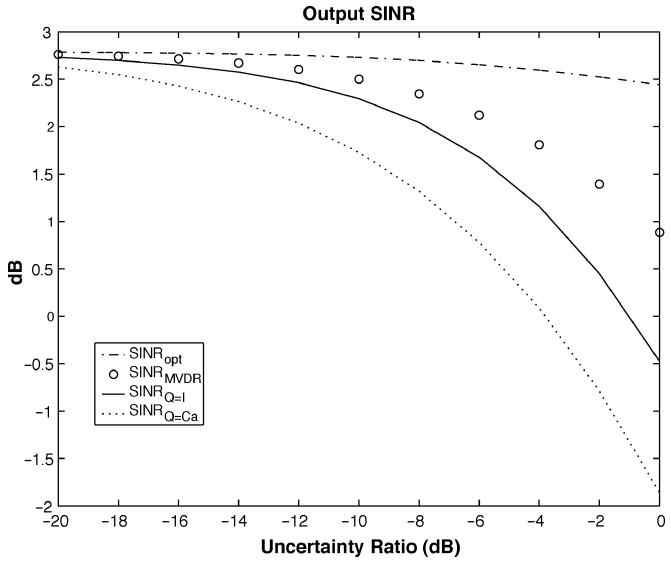

Fig. 7. Case 2—Optimum SINR obtained with the robust beamformer versus uncertainty level. $m = 10$, and SNR $= 3$ dB.

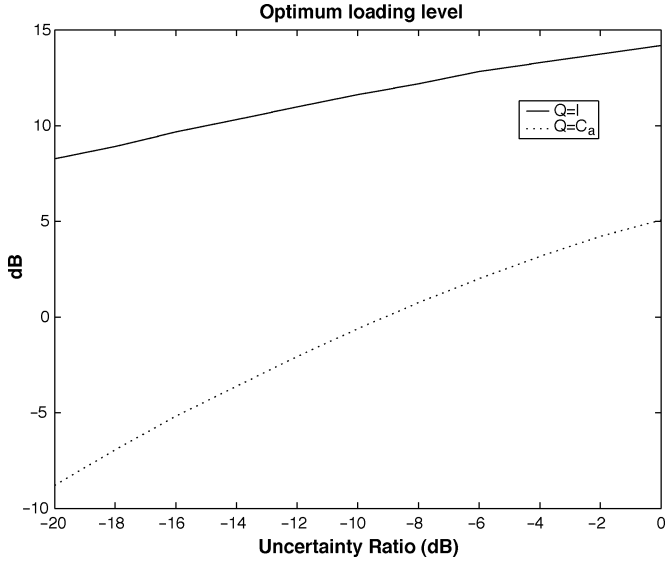

Fig. 8. Case 2—Optimum loading level for the robust beamformer versus uncertainty level. $m = 10$, and SNR $= 3$ dB.

In Figs. 5 and 6, we display the output SINR versus the (array) SNR. In these figures, UR $= -6$ dB, and the loading matrix is still proportional to the identity matrix. We fix the noise level and the loading factor λ is fixed and chosen to be 5 dB above the noise level. The SNR is varied by varying the source power. As can be observed, theoretical and empirical results are still in very good agreement. The diagonally loaded beamformer has a performance close to the MVDR for SNR s below 6 dB. However, it departs from it when SNR increases as λ is fixed and, thus, is no longer chosen optimally.

Finally, we study the influence of the shape of the loading matrix, which is directly related to the form of the ellipsoid in (3). Intuitively, since $\mathcal{E}\{(\boldsymbol{a}-\overline{\boldsymbol{a}})(\boldsymbol{a}-\overline{\boldsymbol{a}})^H\} = \boldsymbol{C}_a$, it follows that $\boldsymbol{a}$ can be written as $\boldsymbol{a} = \overline{\boldsymbol{a}} + \boldsymbol{C}_a^{1/2}\boldsymbol{u}$, where $\boldsymbol{C}_a^{1/2}$ is a square-root of $\boldsymbol{C}_a$. This suggests that $\boldsymbol{B}$ should be related to $\boldsymbol{C}_a^{1/2}$ or, equivalently, that $\boldsymbol{Q} \propto \boldsymbol{C}_a$. Indeed, under the assumption that $\boldsymbol{a}$ is Gaussian distributed, protecting those $\boldsymbol{a} = \overline{\boldsymbol{a}} + \zeta \boldsymbol{C}_a^{1/2}\boldsymbol{u}$ is equivalent to protecting the $\boldsymbol{a}$, which have a given probability of appearance. Hence, we check whether this intuitive hypothesis results in a better performance than using diagonal loading only. Toward this end, we consider the second case only. For each value of UR, we consider both $\boldsymbol{Q} = \lambda \boldsymbol{I}$ and $\boldsymbol{Q} = \lambda \breve{\boldsymbol{C}}_a$ (note that $\mathrm{Tr}\{\breve{\boldsymbol{C}}_a\} = \mathrm{Tr}\{\boldsymbol{I}\}$), and we look for the value of λ that results in the optimal average SINR in (20). We plot in Fig. 7 the obtained optimum SINR and the corresponding loading level in Fig. 8. Examination of these figures reveals two facts. First, as could be expected, the optimum loading level depends on UR (and, of course, on SNR, which is a well-known fact). However, the optimum loading levels vary from one case to another. Second, the performance obtained with $\boldsymbol{Q} \propto \boldsymbol{C}_a$ is always inferior to that obtained with $\boldsymbol{Q} \propto \boldsymbol{I}$. So, even if the steering vector covariance matrix is not a scaled identity matrix, it is questionable

to use something other than diagonal loading. In other words, the use of a flat ellipsoid may not be recommended. Note also, as discussed in [10], that choosing $\boldsymbol{Q} \propto \boldsymbol{C}_a$ implies that one has a strong *a priori* on the shape of the errors, which is seldom the case. Hence, robustness may be endangered if $\boldsymbol{Q}$ is chosen as $\boldsymbol{Q} \propto \boldsymbol{C}_a$, whereas the true covariance matrix of the steering vector errors is not $\boldsymbol{C}_a$. This provides an additional argument in favor of diagonal loading.

V. Conclusions

In this paper, we analyzed the performance of a large class of robust beamformers based on loading of the covariance matrix. The analysis was carried out assuming that random steering vector errors are present. A simple theoretical expression of the output average SINR was derived, which was shown to closely match the results obtained in simulations. Some important conclusions were drawn from this analysis. First, loading of the covariance matrix enables us to maintain a performance close to optimum, at least for small to moderate uncertainties. When the uncertainty ratio is above some level (typically -5 dB), the performance degrades, and one has to turn to other solutions, including estimation of the steering vector. Second, even if the covariance matrix of the steering vector errors is not diagonal, there is no real advantage of using $\boldsymbol{Q} \propto \boldsymbol{C}_a$ instead of $\boldsymbol{Q} \propto \boldsymbol{I}$; hence, conventional diagonal loading, except maybe in some "pathological" cases, turns out to be an effective solution.

Appendix
Proof of (13)

Let $f(.)$ be a (possibly complex-valued) scalar function, and let $\boldsymbol{a} \in \mathbb{C}^m$ be a complex-valued random vector with mean $\overline{\boldsymbol{a}}$. Suppose we wish to calculate the average value of $f(\boldsymbol{a})$

$$\mathcal{E}\{f(\boldsymbol{a})\} = \int f(\boldsymbol{a}) p(\boldsymbol{a}) d\boldsymbol{a} \tag{29}$$

where $p(\boldsymbol{a})$ is the pdf of $\boldsymbol{a}$. For notational convenience, let us define $\boldsymbol{\alpha} = [\boldsymbol{a}_R^T \ \boldsymbol{a}_I^T]^T$ and $\overline{\boldsymbol{\alpha}} = [\overline{\boldsymbol{a}}_R^T \ \overline{\boldsymbol{a}}_I^T]^T$, where the subscripts $_R$ and $_I$ stand for the real and imaginary parts, respectively. Accordingly, let $\boldsymbol{\eta} = [\boldsymbol{a}^T \ \boldsymbol{a}^H]^T$, $\overline{\boldsymbol{\eta}} = \mathcal{E}\{\boldsymbol{\eta}\}$, and $\widetilde{\boldsymbol{\alpha}} = \boldsymbol{\alpha} - \overline{\boldsymbol{\alpha}}$, $\widetilde{\boldsymbol{\eta}} = \boldsymbol{\eta} - \overline{\boldsymbol{\eta}}$, and $\widetilde{\boldsymbol{a}} = \boldsymbol{a} - \overline{\boldsymbol{a}}$. Throughout the Appendix, we adopt the following convention for the derivatives with respect to complex parameters:

$$\frac{\partial}{\partial \boldsymbol{a}} = \frac{1}{2}\left(\frac{\partial}{\partial \boldsymbol{a}_R} + i\frac{\partial}{\partial \boldsymbol{a}_I}\right).$$

Finally, as there cannot be any confusion, we use indifferently $f(\boldsymbol{\alpha})$ or $f(\boldsymbol{a})$. We wish to approximate (29) when the errors are small. In this case, we can write the following Taylor series expansion:

$$\begin{aligned} f(\boldsymbol{a}) &= f(\overline{\boldsymbol{\alpha}}) + \left.\frac{\partial f}{\partial \boldsymbol{\alpha}}\right|_{\overline{\boldsymbol{\alpha}}} \widetilde{\boldsymbol{\alpha}} + \frac{1}{2}\widetilde{\boldsymbol{\alpha}}^T \left.\frac{\partial^2 f}{\partial \boldsymbol{\alpha}\partial \boldsymbol{\alpha}^T}\right|_{\overline{\boldsymbol{\alpha}}} \widetilde{\boldsymbol{\alpha}} + \cdots \\ &= f(\overline{\boldsymbol{a}}) + \widetilde{\boldsymbol{a}}^H \left.\frac{\partial f}{\partial \boldsymbol{a}}\right|_{\overline{\boldsymbol{a}}} + \left.\frac{\partial f}{\partial \boldsymbol{a}^H}\right|_{\overline{\boldsymbol{a}}} \widetilde{\boldsymbol{a}} \\ &\quad + \frac{1}{2}\widetilde{\boldsymbol{\eta}}^T \begin{bmatrix} \left.\frac{\partial^2 f}{\partial \boldsymbol{a}^*\partial \boldsymbol{a}^H}\right|_{\overline{\boldsymbol{a}}} & \left.\frac{\partial^2 f}{\partial \boldsymbol{a}^*\partial \boldsymbol{a}^T}\right|_{\overline{\boldsymbol{a}}} \\ \left.\frac{\partial^2 f}{\partial \boldsymbol{a}\partial \boldsymbol{a}^H}\right|_{\overline{\boldsymbol{a}}} & \left.\frac{\partial^2 f}{\partial \boldsymbol{a}\partial \boldsymbol{a}^T}\right|_{\overline{\boldsymbol{a}}} \end{bmatrix} \widetilde{\boldsymbol{\eta}} + \cdots \end{aligned} \tag{30}$$

Taking the expectation on both sides of the previous equation and ignoring higher order terms, we get

$$\begin{aligned} &\mathcal{E}\{f(\boldsymbol{a})\} \\ &\simeq f(\overline{\boldsymbol{a}}) + \frac{1}{2}\mathrm{Tr}\left\{ \mathcal{E}\{\widetilde{\boldsymbol{\eta}}\widetilde{\boldsymbol{\eta}}^T\} \begin{bmatrix} \left.\frac{\partial^2 f}{\partial \boldsymbol{a}^*\partial \boldsymbol{a}^H}\right|_{\overline{\boldsymbol{a}}} & \left.\frac{\partial^2 f}{\partial \boldsymbol{a}^*\partial \boldsymbol{a}^T}\right|_{\overline{\boldsymbol{a}}} \\ \left.\frac{\partial^2 f}{\partial \boldsymbol{a}\partial \boldsymbol{a}^H}\right|_{\overline{\boldsymbol{a}}} & \left.\frac{\partial^2 f}{\partial \boldsymbol{a}\partial \boldsymbol{a}^T}\right|_{\overline{\boldsymbol{a}}} \end{bmatrix} \right\} \\ &= f(\overline{\boldsymbol{a}}) + \frac{1}{2}\mathrm{Tr}\left\{ \begin{bmatrix} \boldsymbol{\Gamma}_a & \boldsymbol{C}_a \\ \boldsymbol{C}_a^T & \boldsymbol{\Gamma}_a^H \end{bmatrix} \begin{bmatrix} \left.\frac{\partial^2 f}{\partial \boldsymbol{a}^*\partial \boldsymbol{a}^H}\right|_{\overline{\boldsymbol{a}}} & \left.\frac{\partial^2 f}{\partial \boldsymbol{a}^*\partial \boldsymbol{a}^T}\right|_{\overline{\boldsymbol{a}}} \\ \left.\frac{\partial^2 f}{\partial \boldsymbol{a}\partial \boldsymbol{a}^H}\right|_{\overline{\boldsymbol{a}}} & \left.\frac{\partial^2 f}{\partial \boldsymbol{a}\partial \boldsymbol{a}^T}\right|_{\overline{\boldsymbol{a}}} \end{bmatrix} \right\} \\ &= f(\overline{\boldsymbol{a}}) + \mathrm{Tr}\left\{ \boldsymbol{C}_a \left.\frac{\partial^2 f}{\partial \boldsymbol{a}\partial \boldsymbol{a}^H}\right|_{\overline{\boldsymbol{a}}} \right\} \\ &\quad + \frac{1}{2}\mathrm{Tr}\left\{ \boldsymbol{\Gamma}_a \left.\frac{\partial^2 f}{\partial \boldsymbol{a}^*\partial \boldsymbol{a}^H}\right|_{\overline{\boldsymbol{a}}} + \boldsymbol{\Gamma}_a^H \left.\frac{\partial^2 f}{\partial \boldsymbol{a}\partial \boldsymbol{a}^T}\right|_{\overline{\boldsymbol{a}}} \right\} \end{aligned} \tag{31}$$

where $\boldsymbol{\Gamma}_a \triangleq \mathcal{E}\{\widetilde{\boldsymbol{a}}\widetilde{\boldsymbol{a}}^T\}$, $\boldsymbol{C}_a \triangleq \mathcal{E}\{\widetilde{\boldsymbol{a}}\widetilde{\boldsymbol{a}}^H\}$ and where we used the fact that $((\partial^2 f/\partial \boldsymbol{a}^*\partial \boldsymbol{a}^T)|_{\overline{\boldsymbol{a}}})^T = (\partial^2 f/\partial \boldsymbol{a}\partial \boldsymbol{a}^H)|_{\overline{\boldsymbol{a}}}$. When $\boldsymbol{a}$ is circularly symmetric, (31) reduces to

$$\mathcal{E}\{f(\boldsymbol{a})\} \simeq f(\overline{\boldsymbol{a}}) + \mathrm{Tr}\left\{ \boldsymbol{C}_a \left.\frac{\partial^2 f}{\partial \boldsymbol{a}\partial \boldsymbol{a}^H}\right|_{\overline{\boldsymbol{a}}} \right\}. \tag{32}$$

Acknowledgment

The authors wish to thank the reviewers and the Associate Editor for their detailed review, which helped us improve our manuscript.

References

[1] H. V. Trees, *Optimum Array Processing*. New York: Wiley, 2002.
[2] S. Haykin, J. Litva, and T. Shepherd, Eds., *Radar Array Processing*. ser. Springer Series in Information Sciences. Berlin, Germany: Springer-Verlag, 1993.
[3] L. Godara, "Application of antenna arrays to mobile communications, part II: beamforming and direction-of-arrival considerations," *Proc. IEEE*, vol. 85, no. 8, pp. 1195–1245, Aug. 1997.
[4] N. Jablon, "Adaptive beamforming with the generalized sidelobe canceller in the presence of array imperfections," *IEEE Trans. Antennas Propag.*, vol. 34, no. 8, pp. 996–1012, Aug. 1986.
[5] A. Gershman, "Robustness issues in adaptive beamforming and high-resolution direction finding," in *High Resolution and Robust Signal Processing*, Y. Hua, A. Gershman, and Q. Chen, Eds. New York: Marcel Dekker, 2003, ch. 2, pp. 63–110.
[6] Y. I. Abramovich, "Controlled method for adaptive optimization of filters using the criterion of maximum SNR," *Radio Eng. Electron. Phys.*, vol. 26, pp. 87–95, Mar. 1981.
[7] B. Carlson, "Covariance matrix estimation errors and diagonal loading in adaptive arrays," *IEEE Trans. Aerosp. Electron. Syst.*, vol. 24, no. 4, pp. 397–401, Jul. 1988.
[8] D. Manolakis, V. Ingle, and S. Kogon, *Statistical and Adaptive Signal Processing*. New York: McGraw-Hill, 2000.
[9] H. Cox, R. Zeskind, and M. Owen, "Robust adaptive beamforming," *IEEE Trans. Acoust., Speech, Signal Process.*, vol. 35, no. 10, pp. 1365–1376, Oct. 1987.
[10] J. Li, P. Stoica, and Z. Wang, "On robust Capon beamforming and diagonal loading," *IEEE Trans. Signal Process.*, vol. 51, no. 7, pp. 1702–1715, Jul. 2003.
[11] S. Vorobyov, A. Gershman, and Z. Luo, "Robust adaptive beamforming using worst-case performance optimization: a solution to the signal mismatch problem," *IEEE Trans. Signal Process.*, vol. 51, no. 2, pp. 313–324, Feb. 2003.
[12] R. Lorenz and S. Boyd, "Robust minimum variance beamforming," *Proc. Thirty-Seventh Asilomar Conf.*, pp. 1345–1352, Nov. 2003.
[13] I. Reed, J. Mallett, and L. Brennan, "Rapid convergence rate in adaptive arrays," *IEEE Trans. Aerosp. Electron. Syst.*, vol. 10, no. 6, pp. 853–863, Nov. 1974.

[14] R. C. Hanumara, "An alternate derivation of the distribution of the conditioned signal-to-noise ratio," *IEEE Trans. Antennas Propag.*, vol. 34, no. 3, pp. 463–464, Mar. 1986.
[15] C. Khatri and C. Rao, "Effects of estimated noise covariance matrix in optimal signal detection," *IEEE Trans. Acoust., Speech, Signal Process.*, vol. ASSP-35, no. 5, pp. 671–679, May 1987.
[16] R. Monzingo and T. Miller, *Introduction to Adaptive Arrays*. New York: Wiley, 1980.
[17] D. Boroson, "Sample size considerations for adaptive arrays," *IEEE Trans. Aerosp. Electron. Syst.*, vol. 16, no. 4, pp. 446–451, Jul. 1980.
[18] M. Wax and Y. Anu, "Performance analysis of the minimum variance beamformer," *IEEE Trans. Signal Process.*, vol. 44, no. 4, pp. 928–937, Apr. 1996.
[19] ——, "Performance analysis of the minimum variance beamformer in the presence of steering vector errors," *IEEE Trans. Signal Process.*, vol. 44, no. 4, pp. 938–947, Apr. 1996.
[20] C. Richmond, "Derived PDF of maximum likelihood signal estimator which employs an estimated noise covariance," *IEEE Trans. Signal Process.*, vol. 44, no. 2, pp. 305–315, Feb. 1996.
[21] ——, "PDF's, confidence regions, and relevant statistics for a class of sample covariance-based array processors," *IEEE Trans. Signal Process.*, vol. 44, no. 7, pp. 1779–1793, Jul. 1996.
[22] M. Ganz, R. Moses, and S. Wilson, "Convergence of the SMI and the diagonally loaded SMI algorithms with weak interference," *IEEE Trans. Antennas Propag.*, vol. 38, no. 3, pp. 394–399, Mar. 1990.
[23] R. Dilsavor and R. Moses, "Analysis of modified SMI method for adaptive array weight control," *IEEE Trans. Signal Process.*, vol. 41, no. 2, pp. 721–726, Feb. 1993.
[24] L. Fertig, "Statistical performance of the MVDR beamformer in the presence of diagonal loading," in *Proc. First IEEE SAM Workshop*, Cambridge, MA, Mar. 16–17, 2000, pp. 77–81.
[25] M. Viberg and A. Swindlehurst, "Analysis of the combined effects of finite samples and model errors on array processing performance," *IEEE Trans. Signal Process.*, vol. 42, no. 11, pp. 3073–3083, Nov. 1994.
[26] ——, "A Bayesian approach to auto-calibration for parametric array processing," *IEEE Trans. Signal Process.*, vol. 42, no. 12, pp. 3495–3507, Dec. 1994.
[27] S. Shahbazpanahi, A. Gershman, Z.-Q. Luo, and K. Wong, "Robust adaptive beamforming for general-rank signal models," *IEEE Trans. Signal Process.*, vol. 51, no. 9, pp. 2257–2269, Sep. 2003.
[28] G. Fuks, J. Goldberg, and H. Messer, "Bearing estimation in a ricean channel-part I: inherent accuracy limitations," *IEEE Trans. Signal Process.*, vol. 49, no. 5, pp. 925–937, May 2001.

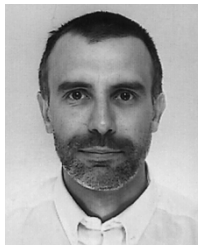

Olivier Besson (M'92–SM'04) received the Ph.D. degree in signal processing in 1992 and the "Habilitation à Diriger des Recherches" degree in 1998, both from INPT, Toulouse, France.

He is currently an Associate Professor with the Department of Avionics and Systems, ENSICA, Toulouse. His research interests are in the general area of statistical signal and array processing with applications in communications and radar.

Dr. Besson served as an Associate Editor for the IEEE TRANSACTIONS ON SIGNAL PROCESSING from Feb. 2000 to January 2003. He is a member of the IEEE SAM Technical Committee and the co-technical chairman of the IEEE SAM04 Workshop.

François Vincent (M'03) received the Engineer and DEA degrees from ENSEEIHT, Toulouse, France, in 1995 and the Ph.D. degree in radar signal processing from the University of Toulouse in 1999.

From 1999 to 2001, he was a research engineer with Siemens, Toulouse. Since 2001, he has been an Assistant Professor with the Departement of Avionics and Systems, ENSICA, Toulouse. His research interests are in array processing and radar.